Journal of Magnetics 12(2), 59-63 (2007)

The Electronic Structures and Magnetism of Monolayer Fe on $CuGaSe_2$(001)

Ying Jiu Jin and Jae Il Lee*

Department of Physics, Inha University, Incheon 402-751, Korea

(Received 4 June 2007)

Ferromagnet/Semiconductor heterostructures have attracted much attention because of their potential applications in spintronic devices. We investigated the electronic structures and magnetism of monolayer Fe on $CuGaSe_2$(001) by using the all-electron full-potential linearized augmented plane-wave method within a generalized gradient approximation. We considered the monolayer Fe deposited on both the CuGa atoms terminated (CuGa-Term) and the Se atom terminated (Se-Term) surfaces of $CuGaSe_2$(001). The calculated magnetic moment of the Fe atom on the CuGa-Term was about 2.90 μ_B. Those of the Fe atoms on the Se-Term were in the range of 2.85-2.98 μ_B. The different magnetic behaviors of the Fe atoms on two different surfaces were discussed using the calculated layer-projected density of states.

Keywords : electronic structures, surface and interface, magnetism, Fe monolayer on $CuGaSe_2$(001), metal-semiconductor junction

1. Introduction

Spintronics, a newly emerging field, includes a development of spin dependent devices such as the spin-polarized field effect transistor (spin-FET), the spin-light emitting diode (spin-LED), and nonvolatile magnetic random access memory (MRAM) devices etc. To make those devices, it is necessary to inject a highly spin-polarized current into semiconductors from ferromagnetic materials.

Ferromagnetic Fe is usually used as a ferromagnetic electrode in a ferromagnet/semiconductor (FM/SC) junction because of the high Curie temperature while the ferromagnetic semiconductors [1, 2] have low Curie temperature. Spin injections in the Fe/ZnSe(001) and Fe/GaAs(001) heterostructures have been investigated by Wunnicke *et al.* [3] using the *ab initio* screened Koringa-Kohn-Rostoker method. They found spin polarization as high as 99% where the interfaces acted as a nearly ideal spin filter. Similar behavior has also been found in the Fe/InAs(001) heterojunction. Zwierzycki *et al.* [4] investigated the spin dependence of the interface resistance of a Fe/InAs(001) heterojunction by the layered tight-binding linear muffin tin orbital (TB-LMTO) surface Green's function method with local density approximation (LDA). They found that the transmitted current polarization was in the range of 98% and 89%, where the specular interface acts as an efficient spin filter. They concluded that efficient spin injection in the Fe/InAs junction could be achieved using high-quality epitaxial interfaces.

In recent years, the successful synthesis of the room temperature ferromagnetic semiconductor, the Mn doped ternary chalcopyrite semiconductor $CdGeP_2$ [5], has encouraged many researchers to exploit the ternary chalcopyrite semiconductors for spintronic applications [6, 7]. Chalcopyrite semiconductors can be classified into two groups: $A^IB^{III}X^{VI}$ type compounds such as $CuGaSe_2$, $CuAlSe_2$, $CuGaS_2$, $CuInS_2$ etc. and the other group, an $A^{II}B^{IV}X^V$ type such as $ZnSiP_2$, $ZnSiAs_2$, $ZnGeP_2$ etc. The crystal structure of the chalcopyrite semiconductor can be regarded as a superlattice of zinc-blende structure; but there are three important structural differences with respect to the zinc-blende structure [8]: (i) the chalcopyrite semiconductors have two types of cations rather than one; (ii) there is a tetragonal distortion of the unit cell with a distortion parameter of $\eta \equiv c/2a \neq 1$; (iii) there are displacements of the anions from the ideal zinc-blende positions with an amount of the u parameter.

One of the chalcopyrite semiconductor, $CuGaSe_2$, has a u parameter of 1/4 as in the regular zinc-blende structure and the η is 0.9825 [9]. There are several structureral and chemical similarities between the $CuGaSe_2$ and GaAs

*Corresponding author: Tel: +82-32-860-7654,
Fax: +82-32-872-7652, e-mail: jilee@inha.ac.kr

semiconductors. The direct band-gap (1.7 eV) [10] of $CuGaSe_2$ is comparable to that (1.54 eV) of the GaAs and both of them have common cation of Ga. The lattice constant (5.61 Å) [9] of $CuGaSe_2$ is very close to that (5.64 Å) of the GaAs.

Many researches have been made to the FM/SC junctions with a binary semiconductor. In this paper, we investigated the electronic structure and magnetism at the interface of ferromagnet and ternary chalcopyrite semiconductor by using the highly precise all-electron FLAPW [11] method within GGA [12]. In Sec. 2, we briefly describe the calculational model and method. We present the results and a discussion on the results in Sec. 3, and we conclude with a brief summary in Sec. 4.

2. Calculational Method

Monolayer Fe on $CuGaSe_2$(001) surfaces was modeled by a Fe monolayer attached on each side of 11 and 9-layer thickness single slabs for the Cu-Ga atoms terminated (CuGa-Term) and the Se atoms terminated (Se-Term), respectively. The schematic top views for the CuGa-Term and Se-Term are illustrated in Fig. 1. A two dimensional (2D) lattice constant was adopted from the experimental lattice constant of 10.61 a.u. [9] The spacing between the Fe monolayer and the $CuGaSe_2$ substrate was assumed to be 2.82 a.u. which was evaluated by keeping the atomic volume as same as that of the bulk bcc iron. We have not optimized the interlayer spacing.

The Kohn-Sham equation [13] was solved self-consistently in terms of the FLAPW method within the GGA to the exchange-correlation potential. Lattice harmonics, with $l \leq 8$, were employed to expand the charge density, potential, and wavefunctions inside the muffin-tin (MT) radius of 2.0 a.u. for the Se atom, 2.2 a.u. for the Fe atom, and 2.4 a.u. for both the Cu and Ga atoms, respectively. An energy cut-off of 12 Ry (corresponding to about 2900 and 2500 LAPW functions for the CuGa-Term and Se-Term, respectively) was employed for the basis set. A 190 Ry star function cut-off was used for depicting the charge density and potential in the interstitial region. Integrations, inside the 2D Brillouin zone (BZ), were replaced by a summation over 12 **k**-points inside the irreducible 2D BZ. All core electrons were treated fully relativistically, while valence states were treated scalar relativistically, i.e., without spin-orbit coupling [14]. Self-consistency was assumed when the difference between input and output charge (spin) densities was less than 1.0×10^{-4} electrons/a.u.^{3}

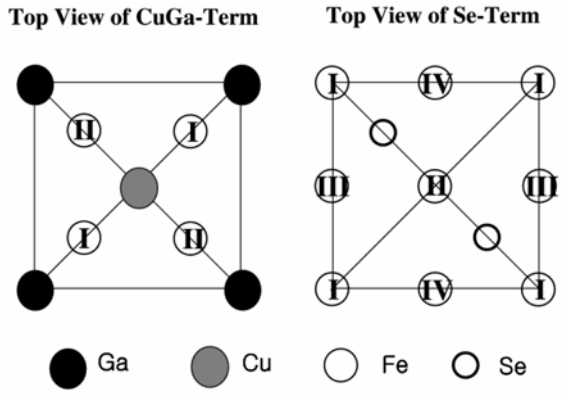

Fig. 1. A schematic top view of the CuGa-Term and Se-Term. The large and small open circles are Fe and Se atoms, respectively. The black and shaded circles are Ga and Cu atoms, respectively. The different types of overlayer Fe atoms are labeled by the Roman numerals.

3. Results and Discussions

The spin density contour plots of the Fe/$CuGaSe_2$(001) in (a) the (110) plane for the CuGa-Term and (b) the (110) plane for Se-Term are presented in Fig. 2. The solid and broken lines represent positively and negatively polarized spin densities, respectively. The lowest contour starts from $\pm5\times10^{-4}$ electrons/a.u.^{3} The subsequent lines differed by a factor of $\sqrt{2}$. As seen from the spin density contour presented in Fig. 2, there was a large eruption of positive spin density toward the vacuum region from the Fe site, which illustrates the large magnetic moments of the overlayer Fe atoms. There are negatively polarized regions which is duo to *sp* electrons between the overlayer Fe and subsurface Cu and Ga atoms for the CuGa-Term, while for the Se-Term the regions between the overlayer Fe and subsurface Se atoms are positively polarized.

The calculated layer by layer magnetic moments (in units of μ_B), as well as the numbers of *l*-decomposed majority and minority spin electrons inside each MT sphere for (a) the CuGa-Term and (b) the Se-Term are tabulated in Table 1.

The magnetic moments of Fe(I) and Fe(II) for the CuGa-Term were calculated to be 2.91 μ_B which was slightly larger than that (2.88 μ_B) of the Fe monolayer on top of the Ga terminated GaAs(001) [14]. The magnetic moments of overlayer Fe atom for the Se-Term were in the range of 2.85-2.98 μ_B. The Fe(IV) had the largest magnetic moment of 2.98 μ_B which was similar to that of the surface layer Fe atom of Fe(001) surface [15], while that of the Fe(III) was the smallest with the value of 2.85 μ_B which was similar to that of Fe monolayer on Cu(001) [16]. The different values of magnetic moments for Fe

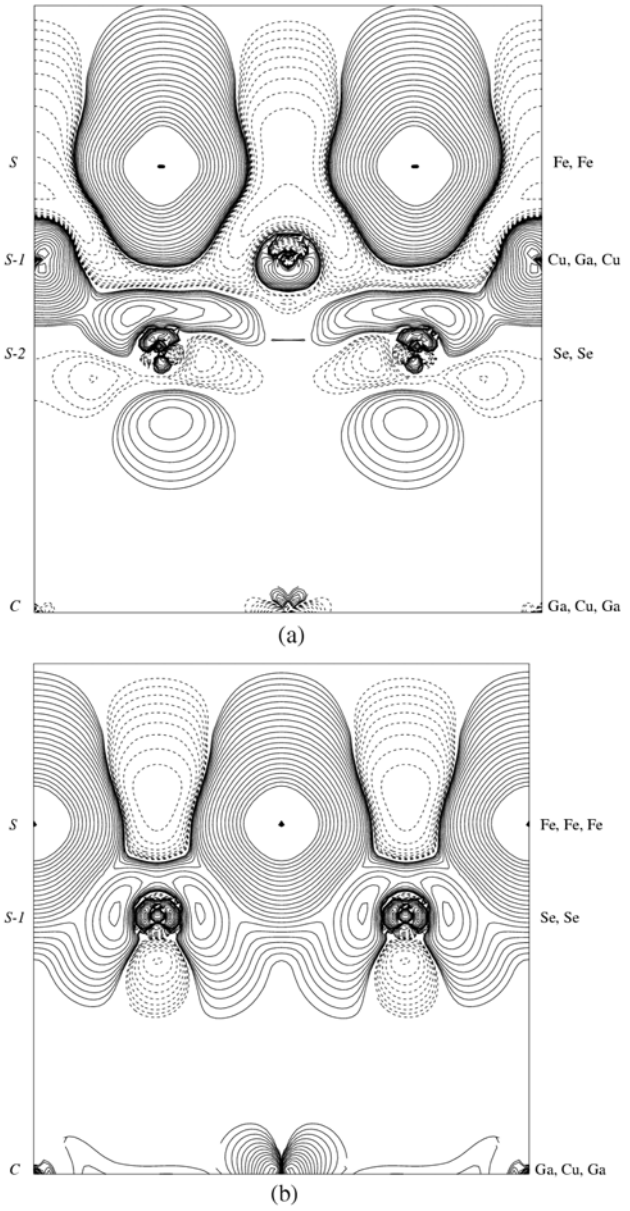

Fig. 2. The spin-density contour plots for (a) the CuGa-Term in the (110) plane and (b) the Se-Term in the (110) plane. The lowest contour starts from $\pm 5 \times 10^{-4}$ electrons/a.u.^{3} and the subsequent lines differ by a factor of $\sqrt{2}$.

atoms indicate that the overlayer Fe magnetic moment is sensitive to its environment as reported by Wu and Freeman [17]. From Fig. 1 we can see that the Fe(III) and Fe(IV) atoms of the Se-Term have one nearest neighbor Se atom with bond lengths of 2.48 Å and four next nearest neighbor Fe atoms with bond lengths of 2.81 Å. However, there is a Ga atom directly below the Fe(III) atom with a distance of 2.87 Å, while the Fe(IV) atom has a Cu atom below it. The magnetic moment of Fe(III) became smaller than that of the Fe(IV) due to the hybridization between Fe(III)-*d* and delocalized Ga-*sp* states.

Table 1. The layer-projected *l*-decomposed majority and minority spin-electrons inside each of the muffin-tin spheres, and layer-by-layer magnetic moments (in units of μ_B).

atom	*s* ↑/↓	*p* ↑/↓	*d* ↑/↓	Total ↑/↓	*M*
CuGa-Term					
Fe(I)	0.16/0.14	0.07/0.08	4.41/1.52	4.65/1.74	2.91
Fe(II)	0.15/0.13	0.08/0.08	4.42/1.53	4.65/1.74	2.91
Cu(*S*-1)	0.25/0.29	0.21/0.23	4.71/4.60	5.20/5.13	0.06
Ga(*S*-1)	0.46/0.48	0.41/0.48	4.99/4.99	5.88/5.97	−0.09
Se(*S*-2)	0.65/0.65	1.00/0.99	4.99/4.99	6.64/6.63	0.01
Cu(*C*)	0.21/0.21	0.20/0.20	4.72/4.72	5.14/5.14	0.00
Ga(*C*)	0.45/0.45	0.40/0.40	5.00/5.00	5.86/5.86	0.00
Se-Term					
Fe(I)	0.12/0.11	0.08/0.08	4.46/1.52	4.68/1.73	2.95
Fe(II)	0.12/0.11	0.08/0.08	4.46/1.52	4.68/1.73	2.95
Fe(III)	0.12/0.12	0.08/0.08	4.44/1.58	4.65/1.79	2.85
Fe(IV)	0.15/0.12	0.07/0.08	4.47/1.51	4.70/1.72	2.98
Se(*S*-1)	0.65/0.65	1.02/0.98	4.99/4.99	6.66/6.62	0.04
Cu(*S*-2)	0.21/0.21	0.20/0.20	4.73/4.71	5.15/5.13	0.03
Ga(*S*-2)	0.48/0.47	0.40/0.39	5.00/5.00	5.89/5.87	0.02
Cu(*C*)	0.21/0.21	0.20/0.20	4.72/4.71	5.15/5.14	0.01
Ga(*C*)	0.45/0.45	0.40/0.40	5.00/5.00	5.86/5.86	0.01

At the interface, there was a small size of induced magnetic moments of 0.06 and −0.09 μ_B for the Cu and Ga atoms of the CuGa-Term, respectively. The Se atom of the Se-Term has a value of 0.04 μ_B.

The microscopic origin of the magnetic behavior of the systems can be seen from the numbers of the *l*-decomposed majority and minority spin electrons inside each MT sphere, given in Table 1. In the MT sphere of Fe atom, the number of *p*-electrons was smaller than that of the bulk, which indicated that the *p*-electrons of the Fe atoms "spill out" into the vacuum region to screen its termination. The numbers of *d*-electrons in each of MT sphere of Fe atom were nearly constants of about 5.95 and 5.98 for the CuGa-Term and Se-Term, respectively. We found that for the CuGa-Term, the interface Cu atoms have small amount of magnetic moment induced by *d*-like electrons, while that of the Ga atoms came from the spin-polarization of *p*-like electrons.

The spin-polarized layer-projected density of states (LDOS) are given in Fig. 3 for (a) the CuGa-Term and (b) the Se-Term, respectively. The solid lines and dotted lines represent majority spins and minority spins, respectively. The Fermi levels (E_F) were set to zero.

For the CuGa-Term, we see that the overall shapes of LDOS of the overlayer Fe(I) and Fe(II) were similar to each other. The majority Fe states had almost a single

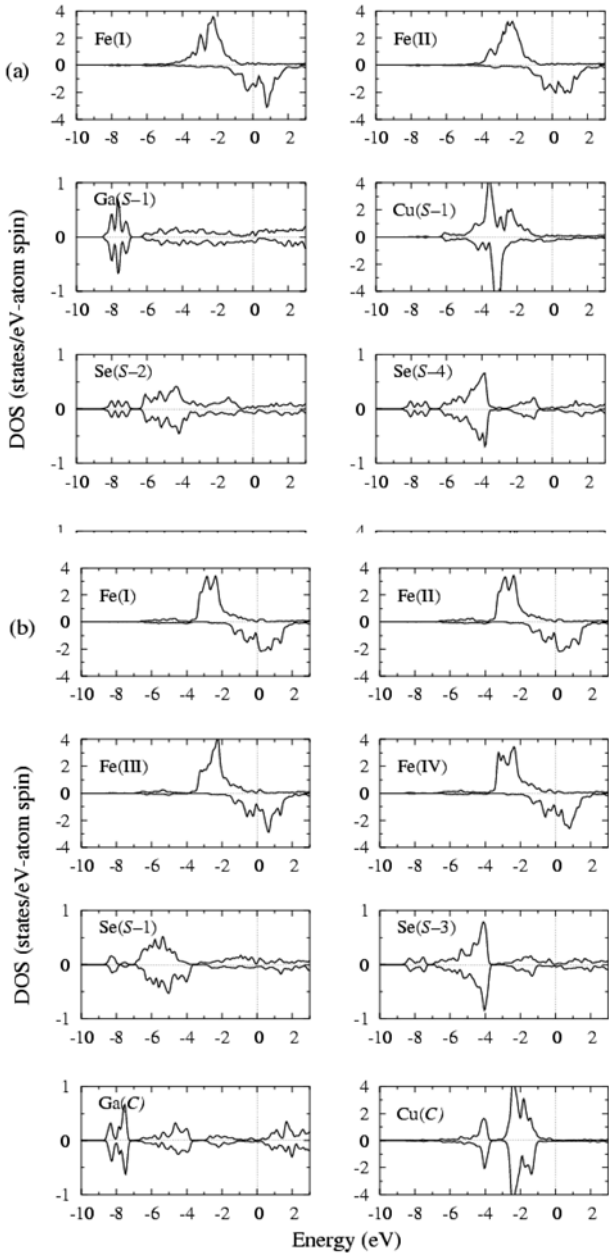

Fig. 3. The spin-polarized layer-projected density of states in (a) the CuGa-Term and (b) the Se-Term. The LDOS values of spin down states are multiplied by −1 and the Fermi levels are set to zero.

main peak. It is found that the substrate Cu *d*-states are dispersed compared to that of center layer Cu atom due to a strong hybridization with the overlayer Fe atoms. The band broadening is also seen in the Ga(*S*-1) atom, which is caused by the *p*-*d* hybridization with the overlayer Fe atoms. On the other hand, the *d*-bands of the overlayer Fe atoms for the Se-Term became more localized with compared to that of the CuGa-Term. This fact is consistent with the larger number of majority Fe *d*-spin electrons for the Se-Term than that for the CuGa-Term as given in Table 1.

4. Summary

We investigated the electronic structures and magnetism of monolayer Fe on $CuGaSe_2$(001) by using the all-electron FLAPW method within GGA. We considered monolayer Fe deposited on both of the CuGa- and Se-terminated surfaces of $CuGaSe_2$(001). The spin densities show a large eruption of positive spin density toward the vacuum region from the overlayer Fe site. The calculated magnetic moments of the overlayer Fe atoms were about 2.91 μ_B for the CuGa-Term, while they were in the range of 2.85-2.98 μ_B for the Se-Term which shows that the magnetism of Fe overlayer is sensitive to the atomic environment. The Fe(IV) of the Se-Term had the largest magnetic moment of 2.98 μ_B, while the magnetic moment of the Fe(III) of the Se-Term was the smallest (2.85 μ_B) due to the Fe(III) *d*- Ga *sp* hybridization with the Ga atom located directly below the Fe(III) atom. The strong hybridization of overlayer Fe *d*-states with the subsurface Cu *d*-, Ga *p*-states for the CuGa-Term induced magnetic moments of 0.06 and −0.09 μ_B on the Cu and Ga atoms, respectively, while the hybridization between the overlayer Fe *d*-states and the Se(*S*-1) *p*-states in the Se-Term induces a smaller magnetic moment (0.04 μ_B) to Se(*S*-1) atom.

References

[1] R. Fiederling, M. Keim, G. Reuscher, W. Ossau, G. Schmidt, A. Waag, and L. W. Molenkamp, Nature (London) **402**, 787 (1999).
[2] Y. Ohno, D. K. Young, B. Beschoten, F. Matdukura, H. Ohno, and D. D. Awschalom, Nature (London) **402**, 790 (1999).
[3] O. Wunnicke, Ph. Mavropoulos, R. Zeller, P. H. Dederichs, and D. Grundler, Phys. Rev. B **65**, 241306 (2002).
[4] M. Zwierzycki, K. Xia, P. J. Kelly, G. E. W. Bauer, and I. Turek, Phys. Rev. B **67**, 092401 (2003).
[5] G. A. Medvedkin, T. Ishibashi, T. Nishi, K. Hayata, Y. Hasegawa, and K. Sato, Jpn. J. Appl. Phys. **39**, L949 (2000).
[6] Y.-J. Zhao and A. J. Freeman, J. Magn. Magn. Mater. **246**, 145 (2002).
[7] S. Cho, S. Choi, G.-B. Cha, S. C. Hong, Y. Kim, Y.-J. Zhao, A. J. Freeman, J. B. Ketterson, B. J. Kim, Y. C. Kim, and B.-C. Choi, Phys. Rev. Lett. **88**, 257203 (2002).
[8] J. E. Jaffe and Alex Zunger, Phys. Rev. **28**, 5822 (1965).
[9] H. W. Spiess, V. Haeberln, G. Brandt, A. Rauber, and J. Schneider, Phys. Stat. Sol. (b) **62**, 183 (1974).

[10] S. Siebentritt, Thin Solid Films **403-404**, 1 (2002).
[11] E. Wimmer, H. Krakauer, M. Weinert, and A. J. Freeman, Phys. Rev. B **24**, 864 (1981), and references therein; M. Weinert, E. Wimmer, and A. J. Freeman, ibid. **26**, 4571 (1982).
[12] J. P. Perdew, K. Burke, and M. Ernzerhof, Phys. Rev. Lett. **77**, 3865 (1996); ibid. **78**, 1396(E) (1997).
[13] W. Kohn and L. J. Sham, Phys. Rev. **140**, A1133 (1965).
[14] (a) D. D. Koelling and B. N. Harmon, J. Phys. C **10**, 3107 (1977). (b) S. S. Kim, S. C. Hong, and J. I. Lee, Phys. Stat. Sol. (b) **189**, 643 (2002).
[15] S. Ohnishi, A. J. Freeman, and M. Weinert, Phys. Rev. B **28**, 6741 (1983).
[16] C. L. Fu and A. J. Freeman, Phys. Rev. B **35**, 925 (1987).
[17] R. Q. Wu and A. J. Freeman, Phys. Rev. B **47**, 3904 (1993).